

Supplementary Materials

Novel Exfoliation of High-Quality 2H-MoS₂ Nanoflakes for Solution-Processed Photodetector

Seulgi Kim ^{1,†}, Woojin Park ^{1,†}, Dohoon Kim ¹, Jiyeon Kang ¹, Jaesoung Lee ¹, Hye Yeon Jang ¹, Sung Ho Song ^{2,*}, Byungjin Cho ^{1,*} and Dongju Lee ^{1,*}

¹ Department of Advanced Materials Engineering, Chungbuk National University, Chungdae-ro 1, Seowon-Gu, Cheongju 28644, Korea; kimsg@chungbuk.ac.kr (S.K.); wjpark80@gmail.com (W.P.); rlaehgns235@gmail.com (D.K.); wldusk0609@chungbuk.ac.kr (J.K.); jaesunglee@cbnu.ac.kr (J.L.); hyjang0581@gmail.com (H.Y.J.)

² Division of Advanced Materials Engineering, Kongju National University, Kongju, Chungnam 330-717, Korea

* Correspondence: shsong805@kongju.ac.kr (S.H.S.); bycho@chungbuk.ac.kr (B.C.); dongjulee@chungbuk.ac.kr (D.L.)

† These authors contributed equally to this work.

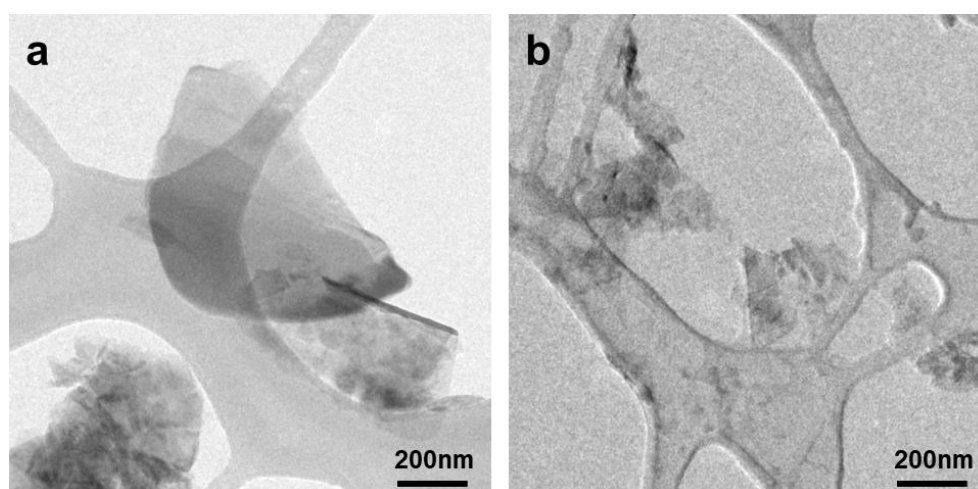


Figure S1. TEM images for MoS₂ NFs with varying rpm. (a) 100 rpm, (b) 300 rpm.

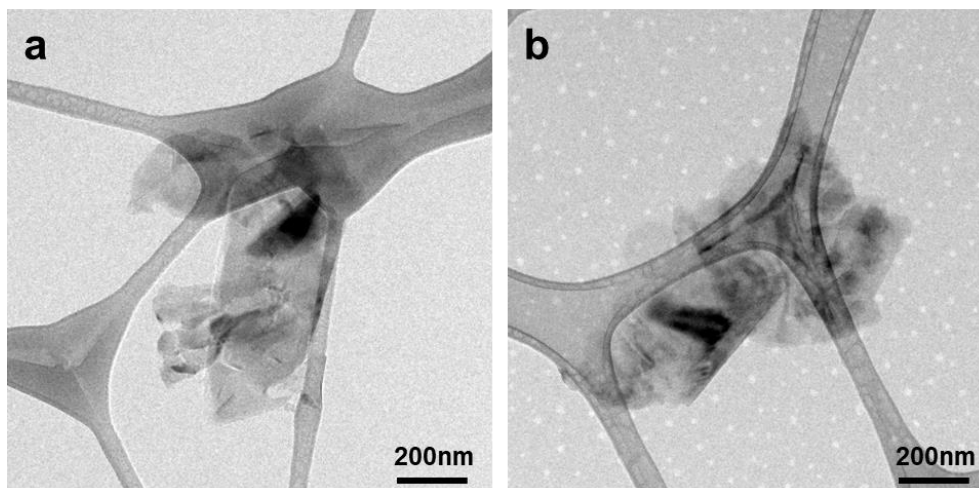


Figure S2. TEM images for MoS₂ NFs according to milling time. (a) 24 hr, (b) 36 hr.

The Raman spectra of the MoS₂ NFs were examined using a 532 nm laser source. Figure S3 shows peaks corresponding to the typical A_{1g} mode and E_{2g} mode of MoS₂ at 407.05 cm⁻¹ and 384.04 cm⁻¹, respectively. A_{1g} mode and E_{2g} mode cause a blue shift and red shift respectively when the number of MoS₂ layers decreases. Thus, the number of MoS₂ layers can be judged by intervals between the peaks of the two modes.

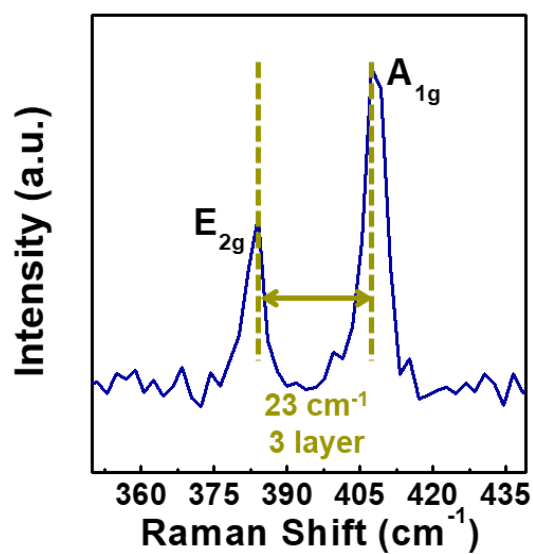


Figure S3. Raman spectra of MoS₂ NFs.

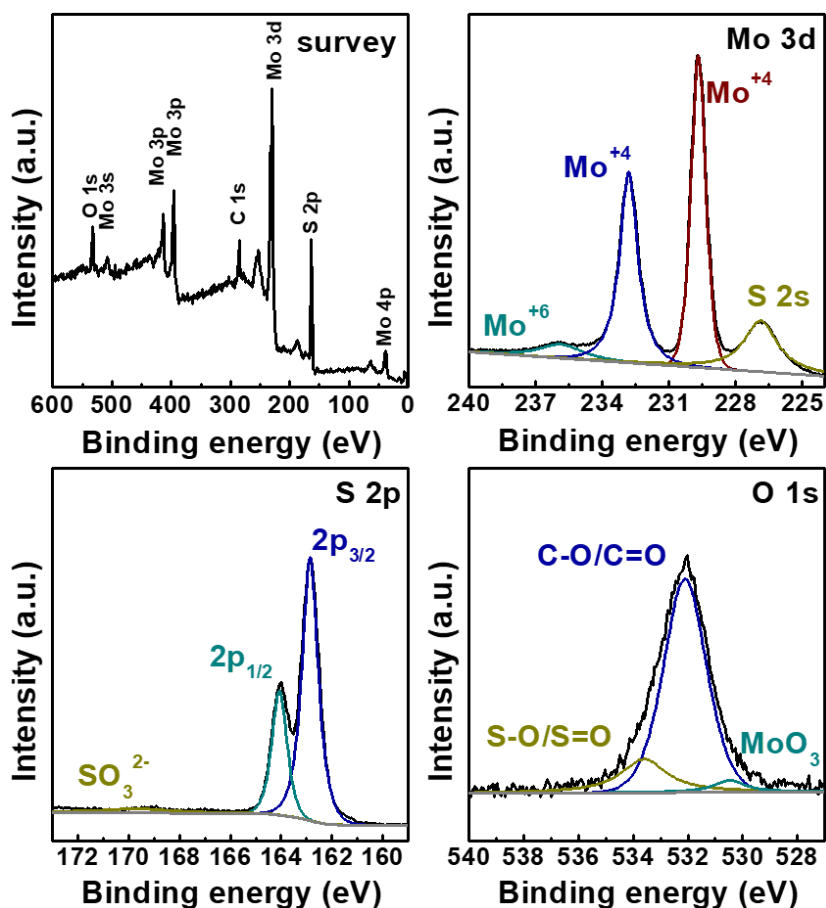


Figure S4. XPS spectra of as-received MoS₂ (a) survey scan, (b) Mo 3d, (c) S 2p and (d) O 1s narrow scan.

Fe residues to be formed during the ball milling process can be confirmed by the Fe narrow scan results in Figure S5b. It is likely that the Fe ion and contaminations perfectly get washed by HCl solution.

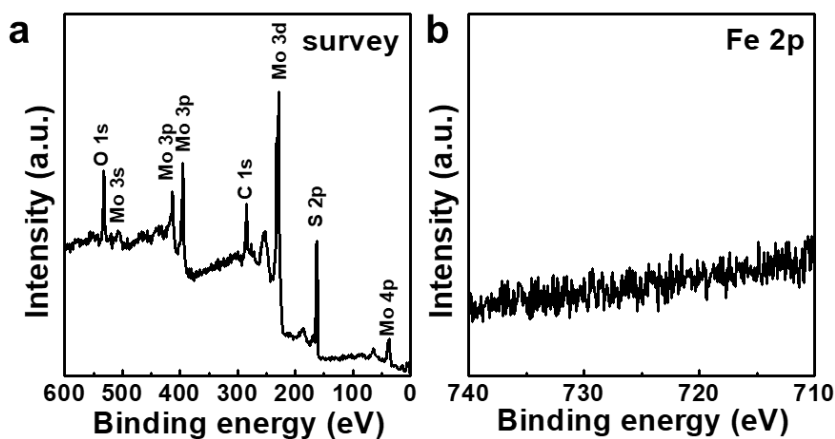


Figure S5. XPS spectra of MoS₂ NFs (a) XPS survey scan, (b) Fe narrow scan.

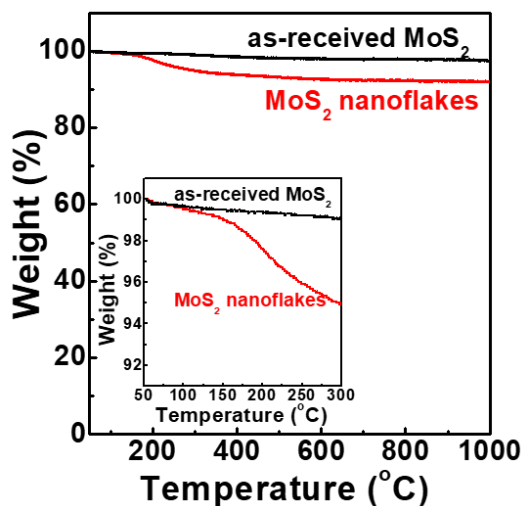


Figure S6. TGA curves at 10°C /min for the thermal decomposition in N₂ atmosphere of MoS₂ NFs.

X-ray diffractometer (XRD) was examined to further identify the crystal structure of MoS₂ NFs. As shown in figure S3, the XRD result show that the MoS₂ NFs have a 2H structure even after the hydrazine-assisted ball milling process. In addition, all peaks became smaller and broader than as-received MoS₂ peaks, indicating that the lateral size of MoS₂ is smaller after exfoliation process.

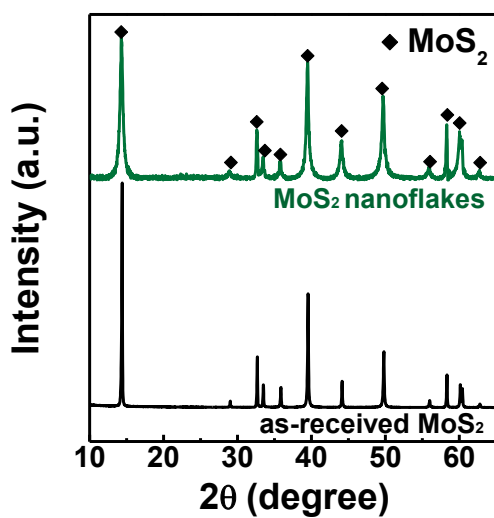


Figure S7. X-ray diffraction pattern of as-received MoS₂ and MoS₂ NFs.

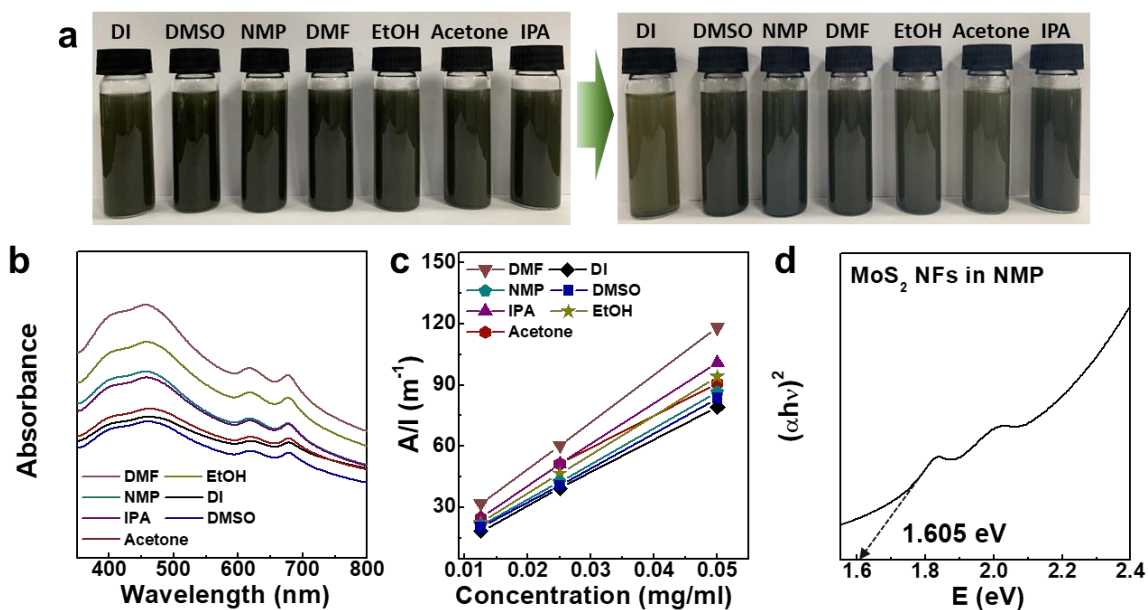


Figure S8. (a) Digital images of MoS₂ NFs suspension in various solvents for 1 week. (b) UV-vis absorption spectrum for MoS₂ NFs. (c) Optical absorbance slopes at excitation wavelength 670 nm as a function of the MoS₂ NFs concentration in each solvent showing Lambert-Beer behavior. (d) Tauc plot of MoS₂ NFs.

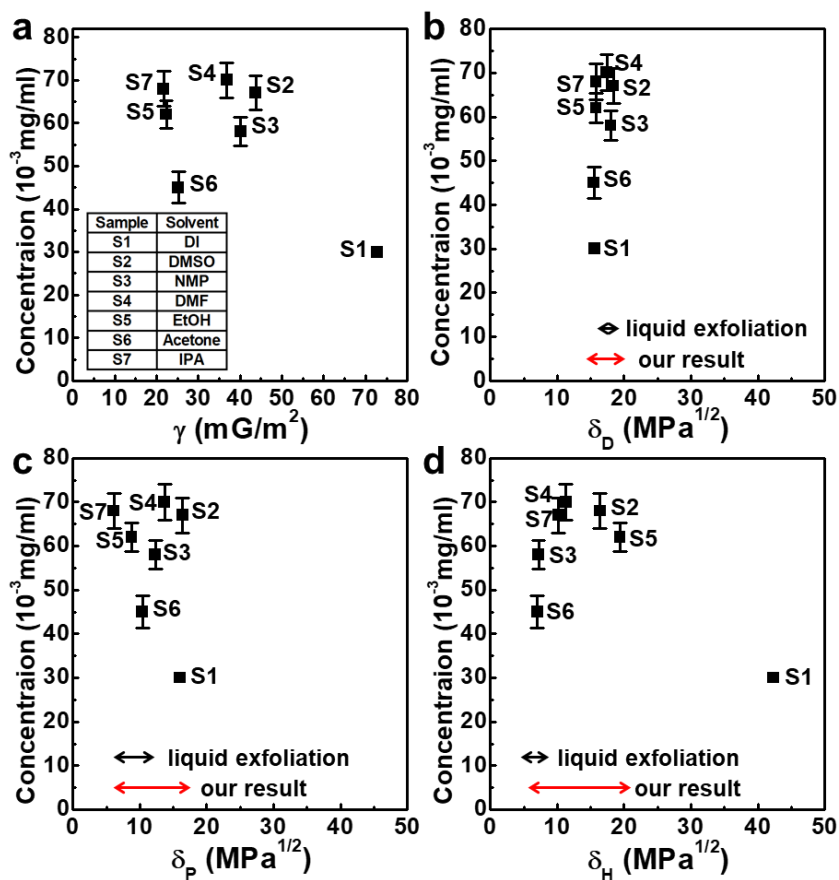


Figure S9. (a) Dispersibility of MoS₂ NFs in various solvents and their surface tension. Dispersion concentration of MoS₂ NFs plotted as a function of the (b) dispersive, (c) polarity, and (d) hydrogen bonding.

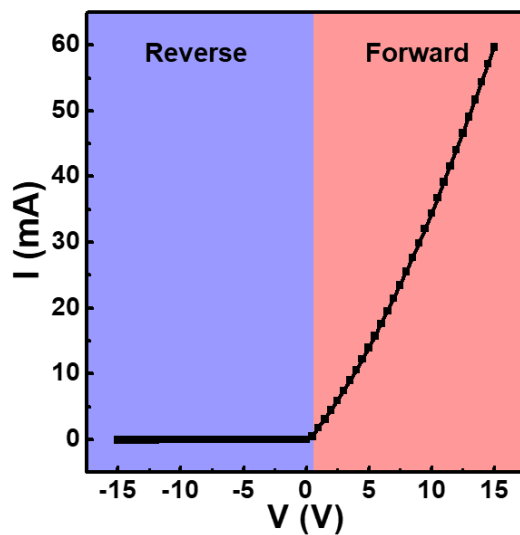


Figure S10. I-V characteristic of MoS₂/p-Si diode.

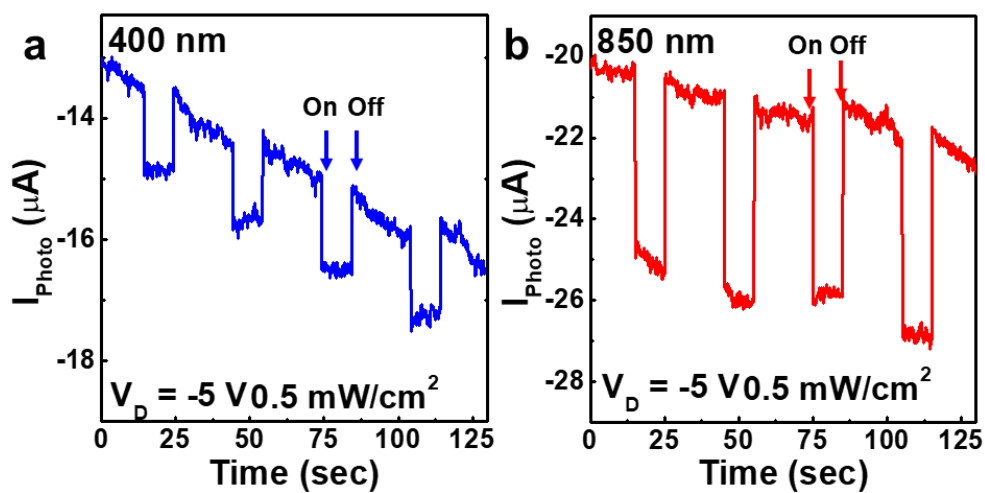


Figure S11. Time-dependent on/off photo current with (a) 400 nm and (b) 850 nm wavelength.